Journal of Environmental Chemical Engineering 14 (2026) 121630

Contents lists available at ScienceDirect

Journal of Environmental Chemical Engineering

journal homepage: www.elsevier.com/locate/jece

Influence of adsorbent composition and solution pH on heavy metal removal from aqueous solution using water treatment residuals from a groundwater treatment plant

Andrea Steuer [a,b], Katharina Sperling [b], Daniel Mahringer [a,*], Aki S. Ruhl [a,b]

[a] Section II 3.3, German Environment Agency (UBA), Schichauweg 58, Berlin 12307, Germany
[b] Water Treatment, Technische Universität Berlin, KF 4, Straße des 17. Juni 135, Berlin 10623, Germany

ARTICLE INFO

Keywords:
Water treatment residuals
Groundwater
Metals
Adsorption
Langmuir
Freundlich

ABSTRACT

The interest in the reuse of water treatment residuals (WTR) as a low-cost alternative to commercial adsorbents for metal removal from aqueous solutions has been growing in recent years. In this study, Fe-WTR and Mn-WTR from a pilot-scale groundwater treatment plant were investigated for their potential to remove As(III), Cd(II), Cu (II), Ni(II) and Pb(II) from different water matrices and at different pH values in batch tests. WTR compositions were compared with chemical and microscopic analyses, revealing that Mn-WTR had a higher Mn content and a slightly higher pH_{PZC} than Fe-WTR. In kinetic experiments at pH 7.0, metal adsorption onto Fe-WTR was faster than adsorption onto Mn-WTR, while final loadings were higher on Mn-WTR. Ni(II) and Cd(II) showed higher affinities for Mn-WTR, while the adsorption capacity of Fe-WTR was exhausted after short contact times. The Elovich model was best suited to describe experimental data, indicating chemisorption as the dominant adsorption mechanism. Isotherm experiments in multi-solute solutions showed that As(III) and Pb(II) removals increased with decreasing pH, while Cd(II) and Ni(II) removals increased with increasing pH. Except for Pb(II), adsorption could be explained with electrostatic interactions between adsorbate and adsorbent, and precipitation likely played a role in metal removal. The Langmuir model described the data better than the Freundlich model in most cases. However, models were unable to represent competition that clearly occurred at higher initial concentrations. Fe-WTR was better suited for metal adsorption in most cases; yet Mn-WTR was more effective for the adsorption of Cd(II) and Ni(II).

1. Introduction

Water treatment residuals (WTR) are waste products that are removed from drinking water treatment filters through flushing. Depending on the type of water treated and the treatment substances used (such as flocculants), WTR are high in metal content such as iron (Fe), aluminium (Al), or manganese (Mn) [1].

During groundwater treatment, soluble Fe(II) and Mn(II) species are oxidized to insoluble Fe(III) and Mn(IV), which remain in subsequent filters as flocs and are removed during filter backwash. The main component of these WTR solids is usually Fe and the percentage is highly dependent on the raw water quality. Recently, WTR have been studied for their use as a cost-efficient alternative to commercial adsorbents for heavy metal removal from aqueous solutions [1–8].

A great variety of adsorbents have been studied for metal removal from water, such as zeolite [9], biochar [10], and layered double hydroxide [11]. Adsorption studies onto WTR have been limited in recent years.

In laboratory settings, such WTR have been studied for removal of Ni [12] and As [13] in single-solute solutions as well as As, Cd, Cu, Pb, Zn, and Cr [6,14] in multi-solute solutions. Fe-WTR has been shown to be an efficient adsorbent for cationic metals with adsorption capacities ranging from 405 mmol/kg (Cd) to 2760 mmol/kg (Zn), depending on the target metal, applied concentrations, and the characteristics of the WTR [6]. Metal adsorption has been reported to depend on pH, adsorbent dose, initial metal concentration, and, in some cases, metal oxidative state [5,6,13,15,16].

Reported removal mechanisms include inner-sphere adsorption, coprecipitation, and precipitation as mineral phases [6]. Some studies evaluating multiple WTR have shown that the composition of the WTR

* Corresponding author.
E-mail address: daniel.mahringer@uba.de (D. Mahringer).

https://doi.org/10.1016/j.jece.2026.121630
Received 5 December 2025; Received in revised form 22 January 2026; Accepted 3 February 2026
Available online 5 February 2026

can impact metal removal [3,6,17].

The use of raw WTR as adsorbents comes with some limitations, such as poor efficiency due to excessive amounts of organic matter and the inability to regenerate used WTR [8]. Different techniques are employed to produce other substances, including thermal modification, acid activation, surface modification and synthesis of composite materials [8]. These modifications usually lead to an increase of the surface area and pore volume [18–20], which in turn can increase adsorption capacity. WTR modification can also lower leaching potential and toxicity [21]. On the other hand, pulverization and granulation can lead to a decrease of surface area and pore volume [22]. Removal of metals using such materials has been studied in storm water [8]. In column tests, removal efficiencies of Fe-WTR coated wood mulches of 88 % for Cu and 92 % for Pb have been reported [23], while thermally treated bentonite-corncob-WTR granules reportedly achieved removal efficiencies of 94 % for Cd, 95 % for Cu, and 98 % for Pb [24]. Studies investigating WTR adsorption of metals from groundwater are scarce and mainly focus on As [8]. Maximum As(III) loading of 3.4 mg/g onto calcium alginated WTR was reported [25].

In surface water treatment, aluminium- and iron-based flocculants are widely used. Consequently, most research has focused on Al- and Fe-based water treatment residuals (Al-WTR and Fe-WTR), as well as adsorbents derived from these materials, for the removal of metals from water. Studies on Mn-based WTR (Mn-WTR), on the other hand, remain limited. This study aims to highlight the potential of Fe-WTR and Mn-WTR generated from a two-stage groundwater treatment plant operating without the addition of flocculants for the removal of As, Cd, Cu, Ni, and Pb from multisolute aqueous solutions. Adsorption kinetics were studied in both drinking water (DW) and ultrapure water (UW) at pH 7.0. The impact of the pH in DW and UW was studied in isotherm batch tests. Common adsorption models were fit to experimental data and relevant model parameters are reported.

2. Material and methods

2.1. Chemicals

For batch tests, As_2O_3 (Alfa Aesar, Haverhill, USA), $CdCl_2 \bullet H_2O$ (Sigma-Aldrich, St. Louis, USA), $CuCl_2 \bullet 2\ H_2O$ (Merck KGaA, Darmstadt, Germany), $NiCl_2 \bullet 6\ H_2O$ (Thermo Fisher Scientific, Waltham, USA), $Pb(CH_3COO)_2 \bullet 3\ H_2O$ (Th. Geyer GmbH & Co. KG, Renningen, Germany) were used. A mixed stock solution was prepared with 10 mg/L of each As (III), Cd(II), Cu(II), Ni(II), Pb(II).

For sample stabilization and analysis, HCl (32 %, Merck KGaA, Darmstadt, Germany), NaOH (Merck KGaA, Darmstadt, Germany), and HNO_3 (65 %, Merck KGaA, Darmstadt, Germany) were used. To buffer pH values during adsorption tests, 0.5 mol/L N,N-bis(2-hydroxyethyl)-2-aminoethanesulfonic acid (BES, pH 6, Alfa Aesar, Haverhill, USA), 0.2 mol/L 2-morpholinoethanesulphonic acid (MES, pH 7, Alfa Aesar, Haverhill, USA) or 0.2 mol/L 3-{[1,3-Dihydroxy-2-(hydroxymethyl) propan.2yl]amino}propane-1-sulfonic acid (TAPS, pH 8 Alfa Aesar, Haverhill, USA) were utilized.

2.2. WTR characterization

WTR were collected from a two-stage groundwater pilot plant optimized for Fe and Mn removal, described in detail by Mahringer et al. [26]. In short, water was treated up-stream in two filters at a filtration velocity of 15 m/h. Both filters were aerated with oxygen separately, and the oxygen concentration was set to predominantly remove Fe in the first filter, and Mn in the second filter. Both filters were backwashed separately with the respective filter effluent for three minutes. Backwash water loss made up approximately 1.3 % of Fe filter throughput and 0.8 % of Mn filter throughput, as Fe filters were flushed more frequently.

WTR were collected during backwash after one minute, as suspended solids concentration was highest at this time point (data not shown). Total suspended solids (TSS) concentrations, which were considered as WTR, were measured according to the respective standard [27] by filtering the backwash water over a pre-rinsed cellulose filter, drying the filter at 105°C for 24 h, and calculating the weight difference before and after drying according to Eq. 1:

$$TSS\left(\frac{g}{L}\right) = \frac{m_{wet} - m_{dried}}{V_{suspension}} \quad (1)$$

m_{wet} = weight of loaded filter before drying (g)
m_{dreid} = weight of loaded filter after drying (g)
$V_{suspension}$ = volume of filtered backwash water (L)

WTR were also dried at 105°C for 24 h and used for the determination of the point of zero charge (pH_{PZC}) using the drift method derived from Tran et al. [28]. 0.01 M NaCl solutions of different pH were prepared by adding HCl or NaOH. Dried WTR were added to set up a concentration of 4 g/L and the final pH value was measured (SenTix® electrode WTW Xylem Analytics, Weilheim, Germany) after shaking (125 rpm) for 24 h. The pH_{PZC} is defined as the pH under which surface charge density is zero, which is observed when the pH does not change over time [28–30]. The same procedure was conducted with fresh WTR in suspension, with a final concentration of 0.01 g/L TSS. Dried WTR were used for surface characterization and to determine the elemental composition using a scanning electron microscope (SEM, Hitachi S-2700, K.K. Hitachi Seisakusho, Tokyo, Japan) equipped with an energy dispersive X-ray (EDX) detector. SEM images were obtained with secondary electrons and back scatter electrons.

WTR compositions were determined by aqua regia digestion according to the respective standard [31]. 0.5 g of WTR were mixed with 2 mL of HNO_3 (63 %) and 6 mL of HCl (32 %). The suspension was heated to 175°C in a microwave (Mars 6, CEM GmbH, Kamp-Lintfort, Germany) and kept at temperature for 10 min. After cooling, samples were filtered over paper and diluted for analysis.

2.3. Batch tests

Kinetic studies for metal adsorption were performed in ultrapure water in polypropylene conic flasks. A pH buffer was added for a final concentration of 0.04 mM. The metal concentrations were set to 1.0 mg/L per metal and pH was set to 7.0 (± 0.1). WTR were added to the pH adjusted metal solutions and samples were shaken between 10 s and 7 days at 125 rpm, and the WTR were removed via filtration (0.45 µm PET filters, Machery-Nagel, Düren, Germany). Samples were prepared in triplicates per timepoint and additional flasks were prepared without WTR addition to determine starting concentrations.

The experimental data was fitted with the pseudo-first-order kinetic model, the pseudo-second-order kinetic model and the Elovich model. Kinetic modelling was done after removal of outliers according to the Dixon test [32,33] in R (version 4.3.2) using RStudio (version 2025.05.1 +513). Goodness of fit was evaluated as outlined in the SI (see Table SI 1).

The pseudo-first-order kinetic model [34] is given in Eq. 2:

$$\frac{dq_t}{dt} = k_1(q_e - q_t) \quad (2)$$

k_1 = rate constant (1/min)
q_e = loading at equilibrium (mg/g)
q_t = loading at contact time t (min)

The pseudo-second-order kinetic model [35] is given in Eq. 3:

$$\frac{dq_t}{dt} = k_2(q_e - q_t)^2 \quad (3)$$

k_2 = rate constant (1/min²)

The Elovich model [36] for chemisorption is given in Eq. 4:

$$\frac{dq_t}{dt} = \alpha e^{-\beta q_t} \quad (4)$$

α = initial adsorption rate (mg/g/min)
β = constant (g/mg)

For isotherm tests, metal solutions at different concentrations (0.01 – 3 mg/L) were prepared in both DW and UW and a pH buffer was added for a concentration of 0.04 mM. To determine the influence of the pH on adsorption, the pH was set to pH 6.0 (± 0.1), 7.0 (± 0.1), or 8.0 (± 0.1) by adding either HCl or NaOH. Lastly, WTR were added from a suspension for a concentration of 0.01 g/L. Samples were shaken for 24 h at 125 rpm and filtered (0.45 µm membranes) at the end of the contact time.

The Langmuir model and the Freundlich model were fitted to the experimental data after outlier removal according to the Dixon test [32, 33] in R using RStudio. The Freundlich model [37] is given in formula 5.

$$q_e = k_f c_e^{\frac{1}{n}} \quad (5)$$

q_e = adsorbent loading at equilibrium (mg/g)
c_e = residual concentration at equilibrium (mg/L)
k_f = Freundlich coefficient (L/g)
$1/n$ = Freundlich exponent (-)

The Langmuir model [38] is given in formula 6.

$$q_e = \frac{q_m k_L c_e}{1 + k_L c_e} \quad (6)$$

q_m = monolayer adsorption capacity (mg/g)
k_L = Langmuir constant (L/g)

All samples containing Fe, Mn, and the target metals were filtered through a 0.45 µm PET syringe filters (Chromafil, Macherey-Nagel, Düren, Germany). Metal samples were acidified with HNO_3 to a final volume concentration of 0.6 %, and metal concentrations were measured using either an ICP-MS (NexION 300 D, Perkin Elmer, Waltham, USA) according to ISO 17294–2 or an ICP-OES (iCap 7000 Seriesm Thermo Fisher Scientific, Waltham, USA). Fe samples were measured immediately using the Spectroquant® test kit 14761 (Merck KGaA, Darmstadt, Germany) and an UV/VIS spectrometer (Lambda 35, Perkin Elmer, Waltham, USA) at a wave length of 562 nm. Mn was measured immediately using the Spectroquant® test kit 114770 (Merck KGaA, Darmstadt, Germany) and a UV/VIS spectrometer at a wave length of 505 nm.

3. Results & discussion

3.1. WTR characterization

TSS concentrations of backwash water samples were determined with 0.8 g/L (n = 5) and 0.2 g/L (n = 4) in Fe and Mn backwash, respectively. As the groundwater used in the pilot plant was higher in Fe (approx. 3.5 mg/L) than Mn (approx. 0.5 mg/L), backwash samples from the Fe removal step were naturally higher in TSS concentration.

The pH_{PZC} was determined by plotting the change of the pH during the experiment over the pH at the start in Fig. 1, with no change in the pH (dashed line) marking the pH_{PZC}. The pH drift behaviour of re-suspended Fe-WTR, re-suspended Mn-WTR and fresh Mn-WTR was similar, with a pH_{PZC} of 8.4 was determined. In contrast, fresh Fe-WTR exhibited a lower pH_{PZC} of 7.1. The pH_{PZC} can decrease due to hydration of oxides and release of weakly bound cations in solution, as was shown previously for manganese hydroxide [39]. These effects might account for the difference in pH_{PZC} between re-suspended Fe-WTR and fresh Fe-WTR. The results suggest that Mn-WTR had a higher positive surface charge than Fe-WTR at pH values between 6.0 and 8.0, whereas Fe-WTR in suspension was likely negative at pH values above 7.1.

The intrinsic metal contents found in WTR as determined using aqua regia digestion, are shown in Table 1. Most metal concentrations measured were below the respective limits of quantification, except for Cu and Pb in Fe-WTR, which were both around 0.5 mg/g. Due to predominant Fe precipitation in the first filter, Fe-WTR were exposed to higher metal concentrations, and consequently, intrinsic loadings of metal on Fe-WTR were higher than on Mn-WTR.

In both WTR, Fe was the most abundant metal detected, as was expected from the high concentrations in the raw water. Mn was the second most abundant metal and Mn concentrations in Mn-WTR were over 35 times higher than in Fe-WTR, resulting in an Fe:Mn mass ratio of approx. 50:1 in Fe-WTR and approx. 1.5:1 in Mn-WTR. The compositional differences arose from the treatment of raw water in the groundwater pilot plant, where Mn is only removed in the second filter, and a controlled breakthrough of Fe through the first filter was allowed.

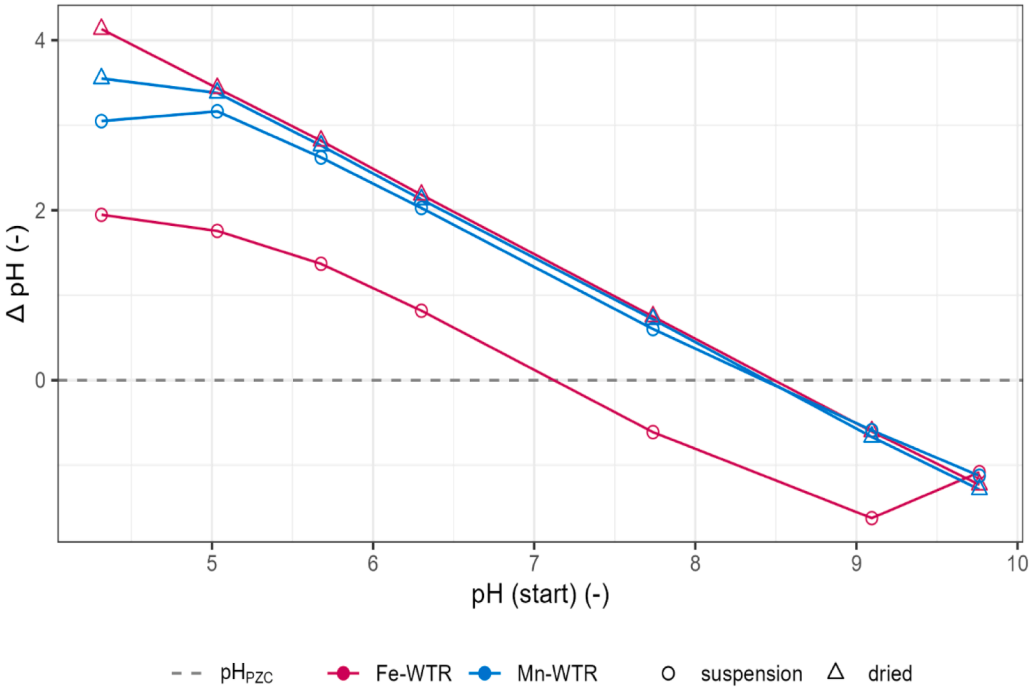

Fig. 1. pH drifts of WTR after addition of fresh (circles) and re-suspended (triangles) WTR to a 0.1 M NaCl solution. The pH_{PZC} is the pH at which no pH drift occurs.

Table 1
Metals in WTR.

WTR	Unit	Fe	Mn	As	Cd	Cu	Ni	Pb
Fe-WTR	mg/g	96.41	1.85	< 0.29	< 0.18	0.56	< 0.26	0.52
Mn-WTR	mg/g	105.96	70.07	< 0.29	< 0.18	< 0.49	< 0.26	< 0.21

SEM images of dried Fe-WTR show a more crystalline surface than images of Mn-WTR, and the particles were generally larger (Fig. 2). Both EDX scans revealed a large oxygen peak indicating oxidized substances (mainly ferric and manganese oxides/hydroxides), and smaller peaks of C, Si, P, and Ca. The semi-quantitative EDX analysis showed the presence of Fe in all samples, with stronger peak intensities in the Fe-WTR sample than the Mn-WTR sample. Mn peaks were clearly detected only in the Mn-WTR. These findings support the results in Table 1, which indicate that Fe is present in both WTR, whereas Mn is predominantly precipitated in the second filter.

3.2. Kinetics of metal adsorption

Metal adsorption curves onto WTR from a multi-solute solution in UW at pH 7.0 as well as model fittings are depicted in Fig. 3. In all cases, a fast initial metal adsorption slowed down with increasing contact time and a final loading was approached asymptotically. This metal adsorption trend was consistent with other experiments [13,16,39–41] and can be attributed to initial bulk adsorption due to a larger concentration differential between the adsorbent surface and the aqueous phase [5]. Initial adsorption onto Fe-WTR was faster than onto Mn-WTR; however final metal loadings were higher on Mn-WTR for all metals except As (III). Ni(II) and Cd(II) adsorption onto Fe-WTR occurred only in the beginning and no further increase of loadings was observed after longer contact times.

Model parameters are summarized in Table 2. The Elovich model, commonly used to describe chemisorption [36], was the best fit according to different goodness of fit calculations in most cases (see Tables SI2 and SI3 in the supporting information). Initial adsorption, as described by the Elovich parameter α, was faster for Fe-WTR than for Mn-WTR. Adsorption kinetics were faster for Fe-WTR in general, as reflected by the rate constants k_1 and k_2 from the pseudo-first-order and pseudo-second-order kinetic models. Calculated loadings on Mn-WTR were higher than on Fe-WTR for most targets (Fig. 3). In the cases of Pb(II) and Ni(II), the pseudo-second-order kinetics model best described the data. Cd(II) adsorption onto Fe-WTR was best described by the

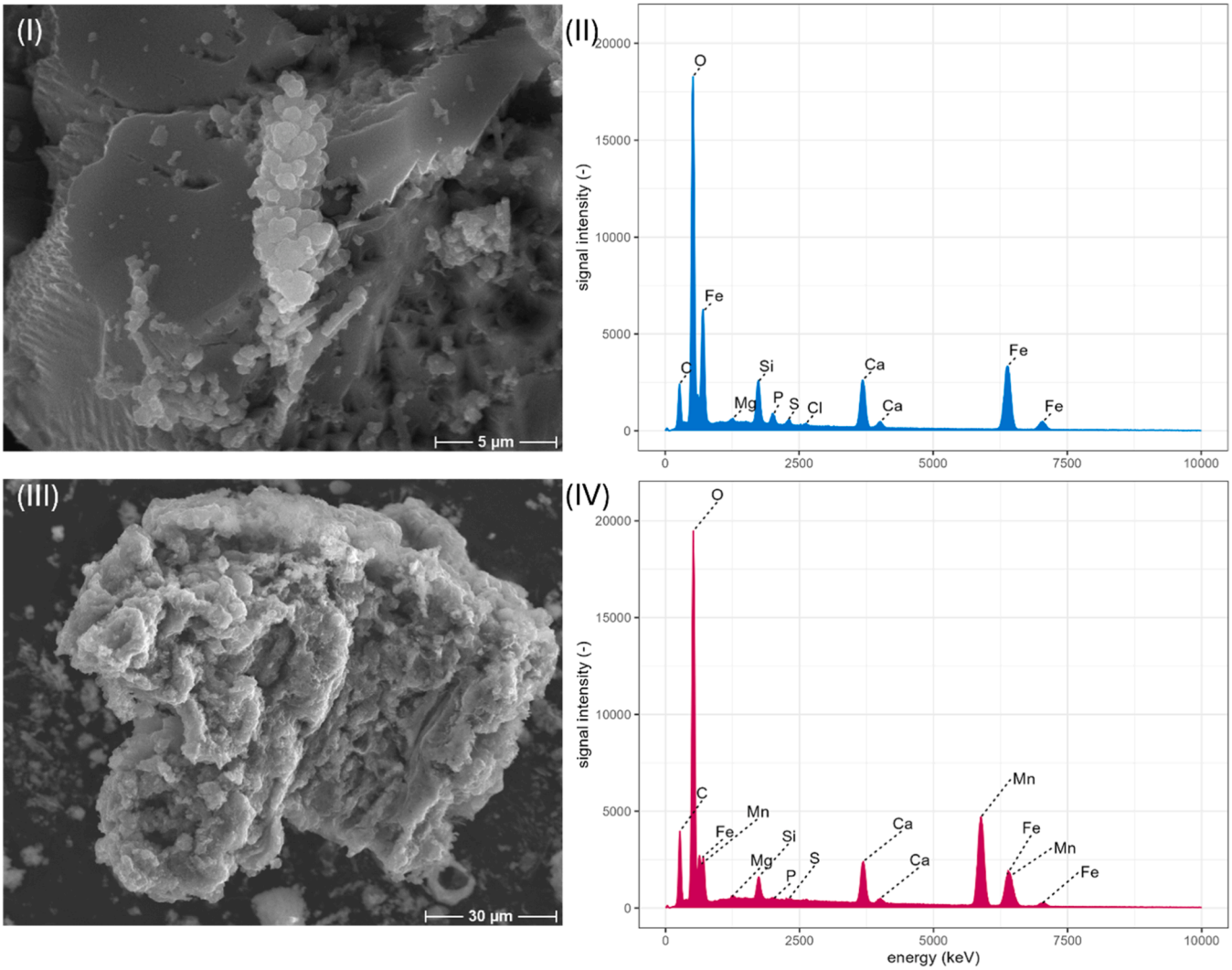

Fig. 2. SEM and EDX analysis of Fe-WTR (I-II) and Mn-WTR (III-IV).

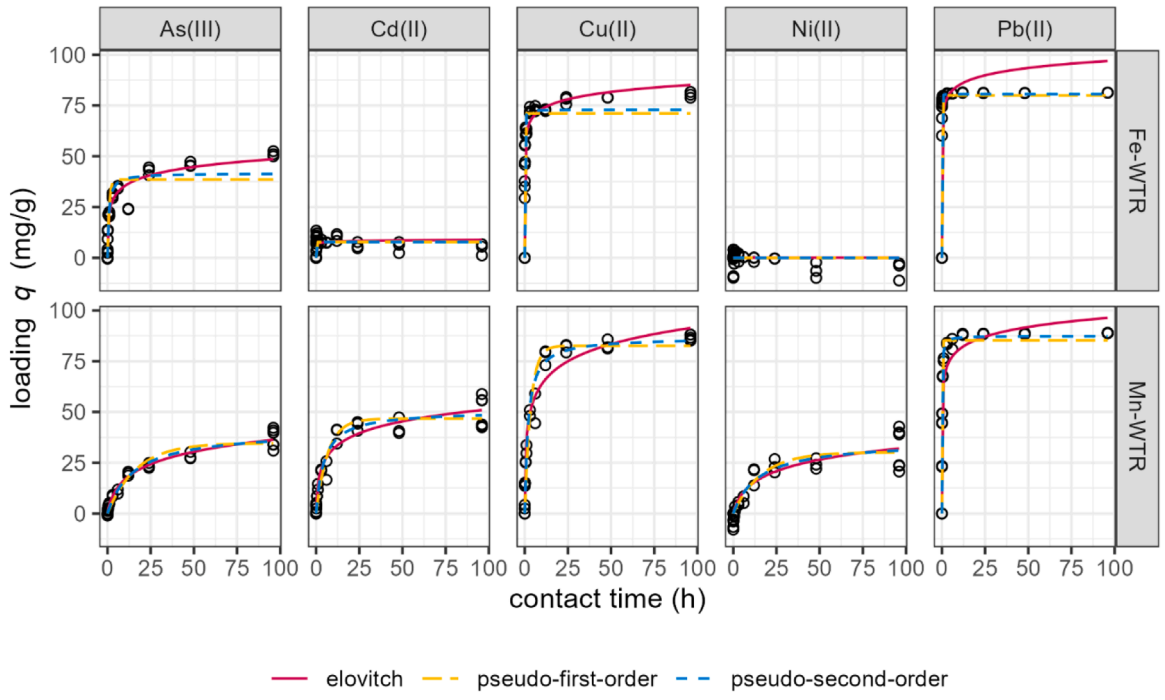

Fig. 3. Adsorption of different metals from a multi-solute solution (1 mg/L per metal) onto Fe-WTR (top) and Mn-WTR (bottom) (each at 0.01 g/L) in UW at pH 7.0. Graphs depict experimental data and model fits.

Table 2
Kinetic parameters derived from the pseudo-first-order kinetic model (PFO), pseudo-second-order kinetic model (PSO) and the Elovich kinetic model. The best-fitting model was chosen based on multiple goodness of fit estimates (see Tables SI2 and SI3).

		PFO		PSO		Elovich		
WTR	**Analyte**	q_e (mg/g)	k_1 (1/min)	q_e (mg/g)	k_2 (mg/g/min)	α (mg/g/min)	β (g/mg)	Best fit
Fe	As	38.5	1.8×10^{-2}	41.6	5.2×10^{-4}	4.2×10^{0}	0.2	Elovich
	Cd	7.8	1.1×10^{0}	7.8	4.5×10^{-1}	1.0×10^{5}	2.4	PFO
	Cu	71.1	2.4×10^{-1}	72.9	6.4×10^{-3}	1.0×10^{4}	0.2	Elovich
	Ni	1×10^{-4}	9.6×10^{-2}	0.1	1.0×10^{-7}	1.0×10^{-2}	100.0	PSO
	Pb	80.0	1.9×10^{0}	80.6	6.2×10^{-2}	1.0×10^{5}	0.2	PSO
Mn	As	34.7	1.0×10^{-3}	41.3	2.6×10^{-5}	7.8×10^{-2}	0.1	Elovich
	Cd	46.7	2.5×10^{-3}	50.7	7.2×10^{-5}	5.8×10^{-2}	0.1	Elovich
	Cu	82.6	4.9×10^{-3}	86.7	1.0×10^{-4}	3.8×10^{0}	0.1	Elovich
	Ni	30.2	1.0×10^{-3}	35.9	3.1×10^{-5}	5.7×10^{-2}	0.1	PSO
	Pb	85.3	1.1×10^{-1}	87.4	1.9×10^{-3}	1.5×10^{3}	0.1	PSO

pseudo-first-order kinetic model. Model fitting for Cd(II) and Ni(II) adsorption onto Fe-WTR was poor and loadings were low, as the adsorption capacity was reached after a short contact time of 30 s. Other metals may have been preferentially adsorbed, causing Cd(II) and Ni(II) to be out-competed by metals with a higher adsorption affinity for Fe-WTR.

3.3. Adsorption isotherms

The influence of pH and water matrix on competitive metal adsorption was studied, and loadings were plotted over residual concentrations along with isotherm model calculations in Fig. 4. For all investigated pH, Pb(II) loadings were roughly one order of magnitude higher than As(III), Cd(II), and Ni(II) loadings, and roughly two to three times as high as Cu(II) loadings, resulting in much lower final solution concentrations. As(III) and Pb(II) adsorption decreased with increasing pH at high initial concentrations, while Cd(II) and Ni(II) adsorption increased with increasing pH. Cu(II) adsorption was highest at pH 7.0 and lowest at pH 8.0. Adsorption of As(III), Pb(II), and Cu(II) was higher onto Fe-WTR, and adsorption of Ni(II) and Cd(II) was higher onto Mn-WTR. By dosing a multi-solute metal solution, competitive adsorption occurred, which is displayed by the sharp decrease in loadings at higher concentrations, especially at pH 8.0, which impacted adsorption of all metal to some extent.

3.4. Influence of pH on metal adsorption

The adsorption of Cd(II) and Ni(II) increased with increasing pH, with maximum loadings of 86 mg/g and 58 mg/g, respectively, at pH 8. Both are present as positive ions (Cd^{2+} and Ni^{2+}) in water at pH values between 6.0 and 8.0 [42]. As WTR surfaces were more negative at higher pH, the electrostatic attraction between both WTR and both metals increased for higher pH. These observations are consistent with published literature [6,16,39,43].

Thermodynamic modelling of As(III) in water indicates it predominantly exists as neutral molecules such as $As(OH)_3$ and $HAsO_2$ below pH 9.0 [44,45]. For this reason, As(III) adsorption is regarded to be independent of pH [13,46]. As(III) can be removed to a high degree by Fe-containing adsorbents including Fe-WTR [13,45–47], with a maximum loading of 62 mg/g. Inner-sphere complexation with hydroxyl groups on the adsorbent surface has been proposed as a removal mechanism [45,47].

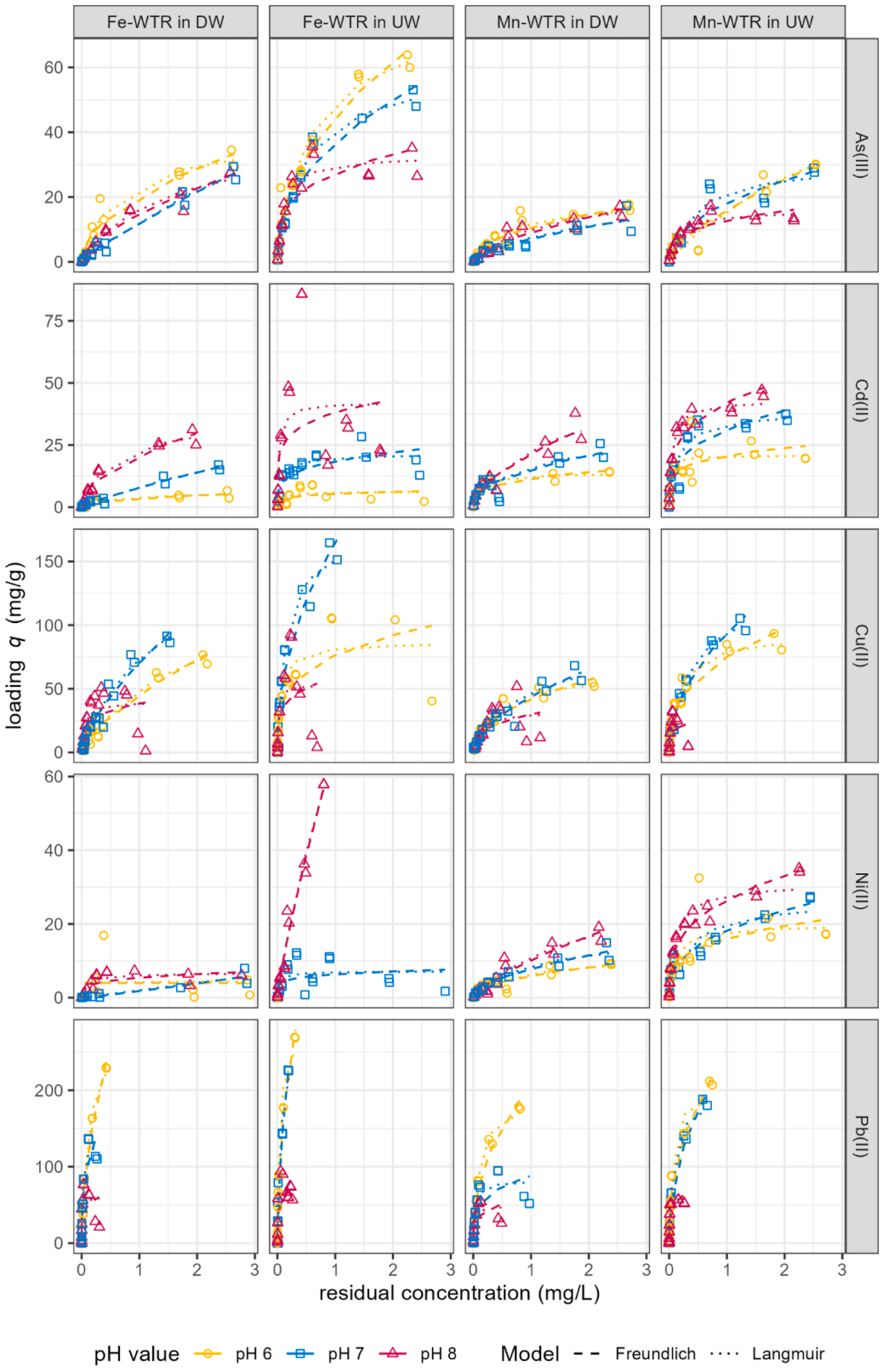

Fig. 4. Loadings in dependence on the water matrix (DW and UP), the WTR (Fe-WTR or Mn-WTR) and pH value (6–8, depicted by colour and shape). Graphs depict data points and isotherms models.

The results of the present study show a minor impact of pH on As(III) adsorption in DW and in UW at low concentrations. However, at higher As(III) concentrations in UW, adsorption decreased considerably for higher pH values, especially onto Fe-WTR. Experimental investigation of this phenomenon exceeded the scope of this study. However, some studies have shown that As(III) might be oxidized to As(V) before adsorption, releasing Mn^{2+} or, under alkaline conditions, Fe^{2+} into the solution [13,48]. In that case and at the investigated pH, As(V) would be

present as the negatively charged species $H_2AsO_4^-$ or $HAsO_4^{2-}$ [44,49]. Several studies have shown that adsorption of As(V) decreased with increasing pH, due to its higher negativity and stronger electrostatic repulsion [13,46,50]. The results presented here show that the pH dependency was more pronounced for Fe-WTR, most likely because its surface charge was more drastically impacted by solution pH. The Fe-WTR surface transitioned from positive to negative between pH 6.0 and 8.0, while the Mn-WTR surface remained positive over this range (Fig. 1), resulting in a stronger electrostatic repulsion of anions from Fe-WTR than Mn-WTR. Future studies on this observation should consider Fe(II) and Mn(II) concentration in the liquid phase and investigate the speciation of adsorbed As, as showcased by Ociński et al. [13], to verify the hypothesized mechanisms.

Pb(II) is present as cations such as Pb^{2+} and $Pb(OH)^+$ under the investigated pH range [44], and can form precipitates (PbO_2, $Pb(OH)_2$, $PbCO_3$) at alkaline pH values and high redox potential [5,44]. Based on electrostatic interactions with the adsorbents' surfaces, which are more positive at lower pH [51], Pb(II) adsorption was expected to increase with increasing pH, as has been shown in other studies [5,39,41,51]. This was not the case in the present study, as Pb(II) loading was highest at pH 6 (269 mg/g). Likely, Pb(II) precipitated as hydroxides [5,39,40], and the resulting Pb precipitates may have been sufficiently small (< 0.45 μm) to pass the membrane filters and partially re-dissolved when the sample was acidified before analysis. The observed decrease of Pb(II) loading with increasing Pb(II) concentration at pH 8.0 could then be explained by increased precipitation due to the exceeded solubility limit.

Cu was expected to be present as cations Cu^+, $CuOH^+$ or Cu^{2+} over the examined pH range [44]. Adsorption was expected to increase for higher pH for both Fe-WTR and Mn-WTR as was observed for Cd(II) and Ni(II). With a maximum loading of 158 mg/g, Cu(II) was best adsorbed at pH 7.0, at which Fe-WTR has a neutral charge and Mn-WTR is slightly positive. At pH 8.0, where Fe-WTR was negatively charged and Mn-WTR was neutral, Cu(II) removal was the lowest. The decrease in Cu(II) adsorption at higher concentrations suggests a strong competition with other cations such as Cd(II) and Ni(II). Cu(II) adsorption has mostly been evaluated at low pH, as precipitation can occur at higher pH [4,40]. Generally, Cu(II) adsorption was described in literature to increase with increasing pH [4,39,40], though Lin et al. [43] observed no pH dependency in UW at pH values between 4.0 and 10.0. El-Kammah et al. [15] observed an increase of adsorption only until the pH_{PZC}, and Likus et al. [6] observed an increase until pH_{PZC} and a drop above pH_{PZC}. Similar to Pb(II), Cu(II) might have been precipitated at high pH and high concentrations and might have passed the membrane filters as colloids, which were re-dissolved after acidification, causing high concentrations in the solutions and low calculated loadings.

3.5. Influence of water matrix on metal adsorption

Maximum loadings were generally higher in UW than DW, indicating competition between DW components and metal for adsorption on WTR. With increasing initial concentrations, Cu(II) loading decreased in DW at pH 8.0 and Pb(II) loadings decreased in DW at pH 7.0 and 8.0. Coexisting ions were not analysed in test waters. DW contains ions such as NO_3^-, Mg^{2+}, SO_4^{2-}, and Ca^{2+}, in concentrations of typically 1.2 – 4.3 mg/L NO_3^-, 8.5 – 12.2 mg/L Mg^{2+}, 64.4 – 152.7 mg/L SO_4^{2-}, and 91.0 – 145.1 mg/L Ca^{2+} [52]. Coexisting ions can compete with metals for available adsorption sites, reducing the activity and interaction of metals with the adsorbent surface, and enhance aggregation of particles by suppression of the electric double layer [53,54]. Furthermore, adsorption of competing ions may alter the surface charge of the adsorbent, thereby affecting electrostatic interactions between the target ions and the surface— for example, the adsorbent surface may become more positive as the amount of adsorbed cations increases [55,56]. Studies on the impact of anions on As(III) adsorption revealed a negative impact of HPO_4^{2-} while NO_3^- and SO_4^{2-} had minor effects [57,58]. Mg^{2+} and Ca^{2+} have been shown to greatly decrease Cd(II) and Cu(II) adsorption while having minor effects on Pb(II) adsorption [53], and an increased ionic strength has been shown to decrease Cu(II) and Ni(II) adsorption [54].

3.6. Influence of WTR characteristics

The WTR differed in composition, with Fe-WTR having a much lower Mn content than Mn-WTR. The pH_{PZC} of Fe-WTR (7.1) was slightly lower than Mn-WTR pH_{PZC} (8.4). At the same pH value, Fe-WTR was therefore expected to be more negative than Mn-WTR, but results did not show improved adsorptions of cations onto Fe-WTR or of anions onto Mn-WTR. As(III) and Pb(II) were adsorbed to a higher degree onto Fe-WTR, while Ni(II), Cd(II) and Cu(II) adsorptions were higher onto Mn-WTR. The affinity of As(III) and Pb(II) for Fe surfaces is well documented [59–62]. Research on the adsorption of metals onto Mn-WTR is scarce, and further investigations need to be conducted to explain the mechanisms that lead to high Cd(II) and Ni(II) adsorption despite the positive surface charge.

Calculated Ni(II) adsorption onto Fe-WTR from UW was below zero at pH 6.0 and at higher concentrations at pH 8.0. This indicates the desorption of Ni(II) from Fe-WTR, which might have been slightly loaded with Ni(II) before the start of the experiment. Ni(II) and Cd(II) adsorption onto Fe-WTR decreased drastically at high initial concentrations in UW at pH 8.0, indicating that both were misplaced due to the adsorption of other cationic metal. This effect was not visible for Mn-WTR, further confirming the preferential adsorption of Ni(II) and Cd (II) onto Mn-WTR.

The use of raw WTR as adsorbents comes with some limitations, such as low affinity and reusability. WTR-based adsorbents come with other drawbacks, such as reduced adsorption capacity through granulation or thermal treatment [22]. WTR produced during the treatment of Fe- and Mn-rich groundwater can be used to remove pollutants in-situ without the need of a further filtration step or any kind of amendment to the WTR. WTR are then removed during regular filter maintenance. For groundwater lacking Fe and Mn, Fe(II) can be added as a suspension in the inflow of the groundwater filter, as has been demonstrated by Mahringer et al. [63] for the removal of vanadium (V(V)). Potentially, Mn(II) could also be added. For technical use, the consistently of WTR quality needs to be studied. While some studies have demonstrated low toxicity and leaching potential of WTR [64,65], these factors would need to be examined closely for in-situ-produced WTR before application and disposal due to the variability of WTR composition.

3.7. Isotherm models of metal adsorption

Langmuir and Freundlich models were fitted to experimental data. Of the 60 data sets considered (each representing a specific combination of analyte, WTR, water matrix, and pH), the Langmuir model provided a better fit in most cases (see Tables SI4 and SI5 and Fig. 3). Based on the Akaike information criterion (AIC) and the sum of squared residuals (RSS), 46 data sets were better fit by the Langmuir model, while R^2 favoured the Langmuir model in 43 cases. Notably, in the three data sets for which R^2 results differed between the AIC and RSS, the R^2 values for both models were nearly identical.

The χ^2 analysis identified 34 data sets as better fit by the Langmuir model. However, the error calculation was affected by negative q_e values in the experimental data, which lead to negative χ^2. Using absolute values of q in the denominator, 52 data sets were better fit by the Langmuir model.

The Langmuir parameter q_{max} estimates the maximum monolayer saturation of the adsorbent [30,66]. The pH value was the most important impact factor on q_{max}. Pb(II) adsorption clearly decreased for higher pH values, while Cu(II) adsorption was highest at pH 7.0 and lowest at pH 8.0. q_{max} values for Ni(II) generally decreased at lower pH. For Cd(II) adsorption, q_{max} was not different at pH 7.0 and 8.0, but lower

at pH 6.0, while no clear link between As(III) adsorption and pH was detected. q_{max} was generally higher in UP than DW. Adsorption onto Fe-WTR was higher in the case of Pb(II), As(III) and Cu(II) than adsorption onto Mn-WTR. There was no clear impact of WTR composition on Cd(II) adsorption, and Ni(II) adsorption onto Mn-WTR was higher than onto Fe-WTR.

The Langmuir constant k_L provides information about the affinity between adsorbent and adsorbate, with lower k_L values (describing a steep initial slope) generally describe a strong affinity [30,66]. As for q_{max}, k_L was most impacted by pH. In the case of Pb(II), k_L increased for higher pH. For Cu(II), k_L was similar at pH 6.0 and pH 7.0, and notably higher at pH 8.0. k_L showed no clear dependency on pH, water matrix, or adsorbent composition in the case of As(III), Cd(II), and Ni(II) adsorption.

The Freundlich exponent $1/n$ describes the adsorption intensity or heterogeneity of the adsorbent surface [13,30,67]. $1/n$ values below 1 indicate favourable adsorption characteristics, while $1/n$ values above 1 indicate unfavourable characteristics [30,56]. $1/n$ was below 1 in most cases, except for Cd(II) and Ni(II) adsorption onto Fe-WTR at pH 7.0. $1/n$ was pH dependent in a few cases. It increased at higher pH in the case of Pb(II) adsorption and did not differ greatly at pH 6.0 and 7.0 for Cu(II) adsorption, but was lowest at pH 8.0. Water matrix had a clear impact on $1/n$ in the cases of As(III) and Cd(II), with $1/n$ being higher in DW than UW. $1/n$ indicated more favourable adsorption onto Mn-WTR than Fe-WTR for the adsorbates Cd(II) and Ni(II).

As the Langmuir model better described the data than the Freundlich model in most cases, the adsorption of the investigated metals onto the WTR was better described by monolayer adsorption than multilayer adsorption [30]. The model parameters, especially q_{max}, did not describe the experimental data accurately in all cases. The competition between the metal strongly influenced the adsorption capacity, but was not considered in these single-solute models. Single-solute isotherm data should be collected for all metals to accurately describe competition. Based on experimental maximum loadings, the adsorption affinity followed the order Pb(II), Cu(II), Cd(II), As(III), Ni(II), while according to Langmuir q_{max}, the order was Ni(II), Pb(II),Cu(II), As (II), Cd(II). Excluding the implausible high q_{max} of Ni(II) adsorption onto Fe-WTR from UW at pH 6.0 (2546 mg/g), which was greatly impacted by negative q values, the affinity order becomes Pb(II), Cu(II), As (II), Cd (II), Ni(II), which is better supported by the experimental data.

4. Conclusions

In this study, two WTR from deep-bed filters for Fe and Mn removals were evaluated for their potential to remove five metals. Both WTR contained large amounts of Fe, while only one contained large amounts of Mn. The pH_{PZC} of the suspended WTR differed, with Mn-WTR being higher at pH_{PZC} 8.4 than Fe-WTR at 7.1. However, after drying and resuspension, both WTR revealed pH_{PZC} around 8.4.

Adsorption kinetics of the target metals from a multi-solute solution onto Fe-WTR were faster than onto Mn-WTR However, final loadings were higher on Mn-WTR. Ni(II) and Cd(II) were adsorbed onto Fe-WTR only at the beginning, and no further increase of loadings was observed for longer contact times, showing clear differences in affinity for the two WTR. The Elovitch model best fit the kinetic data, indicating chemisorption rather than physiosorption.

In isotherm studies, adsorption competition from water components and other metals was apparent, and adsorption was greatly dependent on pH. As(III) and Pb(II) adsorption onto Fe-WTR decreased with increasing pH, with maximum loadings of 62 mg/g and 269 mg/g, respectively. In the case of As(III) adsorption onto Fe-WTR, the pH influence was only clear at high initial concentrations in ultrapure water. Ni(II) and Cd(II) adsorption onto Fe-WTR increased at higher pH values, with maximum loadings of 58 mg/g and 86 mg/g, respectively, at pH 8.0. Cu(II) was best adsorbed onto Fe-WTR at pH 7.0, with a maximum loading of 158 mg/g. Knowledge of the adsorbent pH_{PZC} and surface charge at a given pH was not sufficient to explain WTR affinity for metal adsorption. The Langmuir model was better suited to describe the adsorption data, but the Freundlich and Langmuir model as single-solute models could not accurately describe the competition among the target metals that was apparent from experimental data.

Both examined WTR showed high potential for metal removal. Generally, Fe-WTR was more suited to adsorb metals at the pH range from 6.0 to 8.0, yet Mn-WTR was more favourable for Cd(II) and Ni(II) adsorption. While this study can lay a foundation for the practical use of both WTR, further studies are needed to explain the adsorption mechanisms and affinity of different WTR for different target metals. Further points of interest are the technical feasibility of metal removal alongside Fe and Mn removal, as well as the toxicity and leachability of metals from WTR.

CRediT authorship contribution statement

Andrea Steuer: Writing – review & editing, Writing – original draft, Visualization, Validation, Methodology, Investigation, Formal analysis, Data curation, Conceptualization. **Katharina Sperling:** Writing – review & editing, Investigation, Formal analysis. **Daniel Mahringer:** Writing – review & editing, Validation, Supervision, Methodology, Funding acquisition, Conceptualization. **Aki S. Ruhl:** Writing – review & editing, Supervision, Resources, Project administration, Funding acquisition, Conceptualization.

Declaration of Competing Interest

The authors declare that they have no known competing financial interests or personal relationships that could have appeared to influence the work reported in this paper.

Acknowledgements

This research was funded by the Federal Ministry of Research, Technology and Space as part of the project FITWAS under grant number 02WV1565E and the Federal Ministry of Health under grant number ZMII2–2523FSB460. The authors acknowledge Alexander Kämpfe, Christian Höra and Christoph Merdan of the Umweltbundesamt (UBA) as well as Marcel Hörmann from the Landeswasserversorgung in Langenau for heavy metal measurements and quality control. Sincere thanks go out to Lisa Michael and Sabir Osmani (both UBA) for sample collection and support in the lab.

Appendix A. Supporting information

Supplementary data associated with this article can be found in the online version at doi:10.1016/j.jece.2026.121630.

Data availability

Data will be made available on request.

References

[1] M. Wołowiec, M. Komorowska-Kaufman, A. Pruss, G. Rzepa, T. Bajda, Removal of heavy metals and metalloids from water using drinking water treatment residuals as adsorbents: A review, Minerals 9 (2019) 487, https://doi.org/10.3390/min9080487.

[2] K.A.H. Arab, D.F. Thompson, I.W. Oliver, Evaluation and characterisation of metal sorption and retention by drinking water treatment residuals (WTRs) for environmental remediation, Int. J. Environ. Sci. Technol. 19 (2022) 7727–7736, https://doi.org/10.1007/s13762-021-03674-8.

[3] P. Castaldi, M. Silvetti, G. Garau, D. Demurtas, S. Deiana, Copper(II) and lead(II) removal from aqueous solution by water treatment residues, J. Hazard. Mater. 283 (2015) 140–147, https://doi.org/10.1016/j.jhazmat.2014.09.019.

[4] X. Du, S. Cui, X. Fang, Q. Wang, G. Liu, Adsorption of Cd(II), Cu(II), and Zn(II) by granules prepared using sludge from a drinking water purification plant,

J. Environ. Chem. Eng. 8 (2020) 104530, https://doi.org/10.1016/j.jece.2020.104530.
[5] N.C. Finlay, C.L. Peacock, K.A. Hudson-Edwards, K.L. Johnson, Characteristics and mechanisms of Pb(II) sorption onto Fe-rich waste water treatment residue (WTR): A potential sustainable Pb immobilisation technology for soils, J. Hazard. Mater. 402 (2021) 123433, https://doi.org/10.1016/j.jhazmat.2020.123433.
[6] M. Likus, M. Komorowska-Kaufman, A. Pruss, M. Marzec, T. Bajda, Sorption properties of groundwater treatment residuals containing iron oxides, J. Environ. Chem. Eng. 11 (2023) 110342, https://doi.org/10.1016/j.jece.2023.110342.
[7] R. Nagar, D. Sarkar, K.C. Makris, R. Datta, Effect of solution chemistry on arsenic sorption by Fe- and Al-based drinking-water treatment residuals, Chemosphere 78 (2010) 1028–1035, https://doi.org/10.1016/j.chemosphere.2009.11.034.
[8] S. Sharma, M.M. Ahammed, Application of modified water treatment residuals in water and wastewater treatment: A review, Heliyon 9 (2023) e15796, https://doi.org/10.1016/j.heliyon.2023.e15796.
[9] L. Velarde, M.S. Nabavi, E. Escalera, M.-L. Antti, F. Akhtar, Adsorption of heavy metals on natural zeolites: A review, Chemosphere 328 (2023) 138508, https://doi.org/10.1016/j.chemosphere.2023.138508.
[10] Y. Wang, H. Li, S. Lin, Advances in the study of heavy metal adsorption from water and soil by modified biochar, Water 14 (2022) 3894, https://doi.org/10.3390/w14233894.
[11] X. Feng, R. Long, L. Wang, C. Liu, Z. Bai, X. Liu, A review on heavy metal ions adsorption from water by layered double hydroxide and its composites, Sep. Purif. Technol. 284 (2022) 120099, https://doi.org/10.1016/j.seppur.2021.120099.
[12] D.C. Ong, C.-C. Kan, S.M.B. Pingul-Ong, M.D.G. De Luna, Utilization of groundwater treatment plant (GWTP) sludge for nickel removal from aqueous solutions: Isotherm and kinetic studies, J. Environ. Chem. Eng. 5 (2017) 5746–5753, https://doi.org/10.1016/j.jece.2017.10.046.
[13] D. Ociński, I. Jacukowicz-Sobala, P. Mazur, J. Raczyk, E. Kociołek-Balawejder, Water treatment residuals containing iron and manganese oxides for arsenic removal from water – Characterization of physicochemical properties and adsorption studies, Chem. Eng. J. 294 (2016) 210–221, https://doi.org/10.1016/j.cej.2016.02.111.
[14] Y.W. Chiang, K. Ghyselbrecht, R.M. Santos, J.A. Martens, R. Swennen, V. Cappuyns, B. Meesschaert, Adsorption of multi-heavy metals onto water treatment residuals: Sorption capacities and applications, Chem. Eng. J. 200202 (2012) 405–415, https://doi.org/10.1016/j.cej.2012.06.070.
[15] M. El-Kammah, E. Elkhatib, E. Aboukila, Ecofriendly nanoparticles derived from water industry byproducts for effective removal of Cu (II) from wastewater: Adsorption isotherms and kinetics, Inorg. Chem. Commun. 146 (2022) 110062, https://doi.org/10.1016/j.inoche.2022.110062.
[16] S. Yildiz, S. Sevinç, Heavy metal adsorption by dewatered iron-containing waste sludge, Ecol. Chem. Eng. S 25 (2018) 431–456, https://doi.org/10.1515/eces-2018-0030.
[17] P. Castaldi, E. Mele, M. Silvetti, G. Garau, S. Deiana, Water treatment residues as accumulators of oxoanions in soil. Sorption of arsenate and phosphate anions from an aqueous solution, J. Hazard. Mater. 264 (2014) 144–152, https://doi.org/10.1016/j.jhazmat.2013.10.037.
[18] D. Xu, X. Shi, L.Y. Lee, Z. Lyu, S.L. Ong, J. Hu, Role of metal modified water treatment residual on removal of Escherichia coli from stormwater runoff, Sci. Total Environ. 678 (2019) 594–602, https://doi.org/10.1016/j.scitotenv.2019.04.207.
[19] G. Fu, Y. Zhao, S. Zhou, C. Chen, Y. Zhong, Y. Xu, Efficient removal of nitrogen and phosphorus in aqueous solutions using modified water treatment residuals–sodium alginate beads, Environ. Sci. Pollut. Res 28 (2021) 46233–46246, https://doi.org/10.1007/s11356-021-12586-6.
[20] S. Laib, H. Rezzaz-Yazid, Z. Sadaoui, Comparative study on removal of textile dyes in aqueous medium by adsorption using modified drinking water treatment sludge, Arab J. Sci. Eng. 47 (2022) 6085–6098, https://doi.org/10.1007/s13369-021-05950-8.
[21] M. Wang, S. Bai, X. Wang, Enhanced removal of heavy metals and phosphate in stormwater filtration systems amended with drinking water treatment residual-based granules, J. Environ. Manag. 280 (2021) 111645, https://doi.org/10.1016/j.jenvman.2020.111645.
[22] H.F. Wu, J.P. Wang, E.G. Duan, Y.F. Feng, Z.Y. Wan, Y.X. Wu, Y.Q. Lu, Study on the preparation of granular alum sludge adsorbent for phosphorus removal, Water Sci. Technol. 79 (2019) 2378–2386, https://doi.org/10.2166/wst.2019.241.
[23] V. Sidhu, K. Barrett, D.Y. Park, Y. Deng, R. Datta, D. Sarkar, Wood mulch coated with iron-based water treatment residuals for the abatement of metals and phosphorus in simulated stormwater runoff, Environ. Technol. Innov. 21 (2021) 101214.
[24] M. Wang, S. Bai, X. Wang, Enhanced removal of heavy metals and phosphate in stormwater filtration systems amended with drinking water treatment residual-based granules, J. Environ. Manag. 280 (2021) 111645.
[25] D. Ociński, I. Jacukowicz-Sobala, E. Kociołek-Balawejder, Alginate beads containing water treatment residuals for arsenic removal from water—formation and adsorption studies, Environ. Sci. Pollut. Res 23 (2016) 24527–24539, https://doi.org/10.1007/s11356-016-6768-0.
[26] D. Mahringer, S.S. Zerelli, U. Dippon, A.S. Ruhl, Pilot scale hexavalent chromium removal with reduction, coagulation, filtration and biological iron oxidation, Sep. Purif. Technol. 253 (2020) 117478, https://doi.org/10.1016/j.seppur.2020.117478.
[27] ISO, Ger. Stand. Methods Exam. Water Waste Water Sludge Parameters Charact. Eff. Subst. (Group H.) Determ. Total Dry. Residue Filtr. Dry. Residue Residue ignition (H. 1 (1987), https://doi.org/10.31030/2048062.
[28] H.N. Tran, Y.-F. Wang, S.-J. You, H.-P. Chao, Insights into the mechanism of cationic dye adsorption on activated charcoal: The importance of π–π interactions, Process Saf. Environ. Prot. 107 (2017) 168–180, https://doi.org/10.1016/j.psep.2017.02.010.
[29] G. Newcombe, R. Hayes, M. Drikas, Granular activated carbon: importance of surface properties in the adsorption of naturally occurring organics, Colloids Surf. A Physicochem. Eng. Asp. 78 (1993) 65–71.
[30] H.N. Tran, S.-J. You, A. Hosseini-Bandegharaei, H.-P. Chao, Mistakes and inconsistencies regarding adsorption of contaminants from aqueous solutions: A critical review, Water Res. 120 (2017) 88–116, https://doi.org/10.1016/j.watres.2017.04.014.
[31] ISO, Characterization of sludges - Determination of trace elements and phosphorus - Aqua regia extraction methods, Ger. Version EN 13346 (2001) 2000, https://doi.org/10.31030/9066339.
[32] W.J. Dixon, Ratios Involving Extreme Values, Ann. Math. Stat. 22 (1951) 68–78, https://doi.org/10.1214/aoms/1177729693.
[33] W.J. Dixon, Analysis of extreme values, Ann. Math. Stat. 21 (1950) 488–506.
[34] S. Lagergren, About the theory of so-called adsorption of soluble substances, K. Sven. Vetensk. Handl. (1898) 1–39.
[35] G. Blanchard, M. Maunaye, G. Martin, Removal of heavy metals from waters by means of natural zeolites, Water Res. 18 (1984) 1501–1507, https://doi.org/10.1016/0043-1354(84)90124-6.
[36] I.S. Mclintock, The Elovich equation in chemisorption kinetics, Nature 216 (1967) 1204–1205, https://doi.org/10.1038/2161204a0.
[37] H. Freundlich, Über die Adsorption in Lösungen, Z. F. üR. Phys. Chem. 57 (1907) 385–470.
[38] I. Langmuir, The constitution and fundamental properties of solids and liquids. Part I. Solids, J. Am. Chem. Soc. 38 (1916) 2221–2295.
[39] L. Della Puppa, M. Komárek, F. Bordas, J.-C. Bollinger, E. Joussein, Adsorption of copper, cadmium, lead and zinc onto a synthetic manganese oxide, J. Colloid Interface Sci. 399 (2013) 99–106, https://doi.org/10.1016/j.jcis.2013.02.029.
[40] R. Han, W. Zou, Z. Zhang, J. Shi, J. Yang, Removal of copper(II) and lead(II) from aqueous solution by manganese oxide coated sand, J. Hazard. Mater. 137 (2006) 384–395, https://doi.org/10.1016/j.jhazmat.2006.02.021.
[41] Y.-F. Zhou, R.J. Haynes, Removal of Pb(II), Cr(III) and Cr(VI) from aqueous solutions using alum-derived water treatment sludge, Water Air Soil Pollut. 215 (2011) 631–643, https://doi.org/10.1007/s11270-010-0505-y.
[42] N. Takeno, Atlas of Eh-pH diagrams, Geol. Surv. Jpn. Open File Rep. 419 (2005) 285.
[43] L. Lin, X. Xu, C. Papelis, P. Xu, Innovative use of drinking water treatment solids for heavy metals removal from desalination concentrate: Synergistic effect of salts and natural organic matter, Chem. Eng. Res. Des. 120 (2017) 231–239, https://doi.org/10.1016/j.cherd.2017.02.009.
[44] N. Takeno, Atlas of Eh-pH diagrams, (2005). ⟨https://www.nrc.gov/docs/ML1808/ML18089A638.pdf⟩.
[45] K. Wu, R. Liu, T. Li, H. Liu, J. Peng, J. Qu, Removal of arsenic(III) from aqueous solution using a low-cost by-product in Fe-removal plants—Fe-based backwashing sludge, Chem. Eng. J. 226 (2013) 393–401, https://doi.org/10.1016/j.cej.2013.04.076.
[46] H. Zeng, T. Qiao, Y. Zhao, Y. Yu, J. Zhang, D. Li, Characterization and arsenic adsorption behaviors of water treatment residuals from waterworks for iron and manganese removal, IJERPH 16 (2019) 4912, https://doi.org/10.3390/ijerph16244912.
[47] K.C. Makris, D. Sarkar, J.G. Parsons, R. Datta, J.L. Gardea-Torresdey, Surface arsenic speciation of a drinking-water treatment residual using X-ray absorption spectroscopy, J. Colloid Interface Sci. 311 (2007) 544–550, https://doi.org/10.1016/j.jcis.2007.02.078.
[48] G.-S. Zhang, J.-H. Qu, H.-J. Liu, R.-P. Liu, G.-T. Li, Removal mechanism of As(III) by a novel Fe−Mn binary oxide adsorbent: oxidation and sorption, Environ. Sci. Technol. 41 (2007) 4613–4619, https://doi.org/10.1021/es063010u.
[49] J.A. Cherry, A.U. Shaikh, D.E. Tallman, R.V. Nicholson, Arsenic species as an indicator of redox conditions in groundwater. Developments in Water Science, Elsevier, 1979, pp. 373–392, https://doi.org/10.1016/S0167-5648(09)70027-9.
[50] K. Wu, T. Liu, J.M. Peng, Adsorption behaviors of arsenic(V) onto Fe-based backwashing sludge produced from Fe(II)-removal plants, Appl. Mech. Mater. 295298 (2013) 1321–1326, https://doi.org/10.4028/www.scientific.net/AMM.295-298.1321.
[51] R. Duan, C.B. Fedler, Competitive adsorption of Cu2+, Pb2+, Cd2+, and Zn2+ onto water treatment residuals: implications for mobility in stormwater bioretention systems, Water Sci. Technol. 86 (2022) 878–893, https://doi.org/10.2166/wst.2022.258.
[52] Berliner Wasserbetriebe, Wasserqualität - Analysedaten nach Postleitzahl, (2023). ⟨https://www.bwb.de/de/analysedaten-nach-postleitzahlen.php?PLZ=12307&send=Suche+starten⟩ (accessed May 8, 2025).
[53] W. Liu, T. Wang, A.G.L. Borthwick, Y. Wang, X. Yin, X. Li, J. Ni, Adsorption of Pb2+, Cd2+, Cu2+ and Cr3+ onto titanate nanotubes: Competition and effect of inorganic ions, Sci. Total Environ. 456457 (2013) 171–180, https://doi.org/10.1016/j.scitotenv.2013.03.082.
[54] T. Musso, M. Parolo, G. Pettinari, pH, ionic strength, and ion competition effecton Cu(II) and Ni(II) sorption by a Na-bentonite used as liner material, Po, l. J. Environ. Stud. 28 (2019) 2299–2309, https://doi.org/10.15244/pjoes/84922.
[55] D.C. Ong, S.M.B. Pingul-Ong, C.-C. Kan, M.D.G. De Luna, Removal of nickel ions from aqueous solutions by manganese dioxide derived from groundwater treatment sludge, J. Clean. Prod. 190 (2018) 443–451, https://doi.org/10.1016/j.jclepro.2018.04.175.

[56] H. Zeng, Y. Yu, F. Wang, J. Zhang, D. Li, Arsenic(V) removal by granular adsorbents made from water treatment residuals materials and chitosan, Colloids Surf. A Physicochem. Eng. Asp. 585 (2020) 124036, https://doi.org/10.1016/j.colsurfa.2019.124036.
[57] P. Khownpurk, W. Chandra-Ambhorn, As(III) removal under the presence of competitive anions using the calcined ground oyster shell as the adsorbent, Sep. Sci. Technol. 55 (2020) 395–405, https://doi.org/10.1080/01496395.2019.1577269.
[58] T. Tuutijärvi, E. Repo, R. Vahala, M. Sillanpää, G. Chen, Effect of competing anions on arsenate adsorption onto maghemite nanoparticles, Chin. J. Chem. Eng. 20 (2012) 505–514, https://doi.org/10.1016/S1004-9541(11)60212-7.
[59] R. Bhateria, R. Singh, A review on nanotechnological application of magnetic iron oxides for heavy metal removal, J. Water Process Eng. 31 (2019) 100845, https://doi.org/10.1016/j.jwpe.2019.100845.
[60] D.E. Giles, M. Mohapatra, T.B. Issa, S. Anand, P. Singh, Iron and aluminium based adsorption strategies for removing arsenic from water, J. Environ. Manag. 92 (2011) 3011–3022, https://doi.org/10.1016/j.jenvman.2011.07.018.
[61] L. Hao, M. Liu, N. Wang, G. Li, A critical review on arsenic removal from water using iron-based adsorbents, RSC Adv. 8 (2018) 39545–39560, https://doi.org/10.1039/C8RA08512A.
[62] C. Zhang, Z. Yu, G. Zeng, B. Huang, H. Dong, J. Huang, Z. Yang, J. Wei, L. Hu, Q. Zhang, Phase transformation of crystalline iron oxides and their adsorption abilities for Pb and Cd, Chem. Eng. J. 284 (2016) 247–259, https://doi.org/10.1016/j.cej.2015.08.096.
[63] D. Mahringer, S.S. Zerelli, A.S. Ruhl, Pilot-scale vanadium adsorption onto in-situ biogenic amorphous ferric hydroxide, J. Water Process Eng. 56 (2023) 104278, https://doi.org/10.1016/j.jwpe.2023.104278.
[64] L. Zhou, S.M. Wallace, N.D. Denslow, J.-F. Gaillard, P. Meyer, J.-C.J. Bonzongo, A screening approach for the selection of drinking water treatment residuals for their introduction to marine systems, Environ. Toxicol. Chem. 40 (2020) 1194–1203, https://doi.org/10.1002/etc.4950.
[65] L. Zhou, S.M. Wallace, K.J. Kroll, N.D. Denslow, J.-F. Gaillard, P. Meyer, J.-C. J. Bonzongo, Acute and chronic toxicity testing of drinking water treatment residuals in freshwater systems, Environ. Toxicol. Chem. 40 (2021) 2003–2012, https://doi.org/10.1002/etc.5061.
[66] D. Kratochvil, Advances in the biosorption of heavy metals, Trends Biotechnol. 16 (1998) 291–300, https://doi.org/10.1016/S0167-7799(98)01218-9.
[67] M.D.G. De Luna, E.D. Flores, D.A.D. Genuino, C.M. Futalan, M.-W. Wan, Adsorption of Eriochrome Black T (EBT) dye using activated carbon prepared from waste rice hulls—Optimization, isotherm and kinetic studies, J. Taiwan Inst. Chem. Eng. 44 (2013) 646–653, https://doi.org/10.1016/j.jtice.2013.01.010.